EUROPEAN ORGANIZATION FOR NUCLEAR RESEARCH
CERN - ACCELERATORS AND TECHNOLOGY SECTOR

CERN-ATS-2012-033

Design of 11 T Twin-Aperture Nb_3Sn Dipole Demonstrator Magnet for LHC Upgrades

M. Karppinen[1], N. Andreev[2], G. Apollinari[2], B. Auchmann[1], E. Barz[2]i, R. Bossert[2], V.V. Kashikhin[2], A. Nobrega[2], I. Novitski[2], L. Rossi[1], D. Smekens[1], A.V. Zlobin[2]
1 CERN, Geneva, Switzerland
2 Fermilab National Accelerator Laboratory, Batavia, USA

Abstract

The LHC collimation upgrade foresees two additional collimators installed in the dispersion suppressor regions of points 2, 3 and 7. To obtain the necessary longitudinal space for the collimators, a solution based on an 11 T dipole as replacement of the 8.33 T LHC main dipoles is being considered. CERN and FNAL have started a joint development program to demonstrate the feasibility of Nb_3Sn technology for this purpose. The program started with the development and test of a 2-m-long single-aperture demonstrator magnet. The goal of the second phase is the design and construction of a series of 2-m-long twin-aperture demonstrator magnets with a nominal field of 11 T at 11.85 kA current. This paper describes the electromagnetic design and gives a forecast of the field quality including saturation of the iron yoke and persistent-current effects in the Nb_3Sn coils. The mechanical design concepts based on separate collared coils, assembled in a vertically split iron yoke are also discussed.

This work was supported in part by Fermi Research Alliance, LLC, under contract No. DE-AC02-07CH11359 with the U.S. Department of Energy.

Presented at the 22nd International Conference on Magnet Technology (MT-22)
12-16 September 2011, Marseille, France

Geneva, Switzerland

February 2012

Design of 11 T Twin-Aperture Nb_3Sn Dipole Demonstrator Magnet for LHC Upgrades

M. Karppinen, N. Andreev, G. Apollinari, B. Auchmann, E. Barzi, R. Bossert, V.V. Kashikhin, A. Nobrega, I. Novitski, L. Rossi, D. Smekens, A.V. Zlobin

***Abstract*—The LHC collimation upgrade foresees two additional collimators installed in the dispersion suppressor regions of points 2, 3 and 7. To obtain the necessary longitudinal space for the collimators, a solution based on an 11 T dipole as replacement of the 8.33 T LHC main dipoles is being considered. CERN and FNAL have started a joint development program to demonstrate the feasibility of Nb_3Sn technology for this purpose. The program started with the development and test of a 2-m-long single-aperture demonstrator magnet. The goal of the second phase is the design and construction of a series of 2-m-long twin-aperture demonstrator magnets with a nominal field of 11 T at 11.85 kA current. This paper describes the electromagnetic design and gives a forecast of the field quality including saturation of the iron yoke and persistent-current effects in the Nb_3Sn coils. The mechanical design concepts based on separate collared coils, assembled in a vertically split iron yoke are also discussed.**

***Index Terms*—Accelerator magnet, Nb_3Sn, Twin-aperture dipole.**

I. INTRODUCTION

THE second phase of the LHC collimation upgrade will enable proton and ion beam operation at nominal and ultimate intensities. To improve the collimation efficiency by a factor 15-90, additional collimators are foreseen in the room temperature insertions and in the dispersion suppression (DS) regions around points 2, 3, and 7 [1].

To provide longitudinal space of about 3.5 m for additional collimators, a solution based on the substitution of a pair of 5.5-m-long 11 T dipoles for several 14.3-m-long 8.33 T LHC main dipoles (MB) [2] is being considered. These twin-aperture dipoles operating at 1.9 K shall be powered in series with the main dipoles and deliver the same integrated strength of 119 Tm at the nominal current of 11.85 kA.

After the initial pre-study [3], CERN and FNAL started a joint development program with the goal of building a 5.5-m-long twin-aperture Nb_3Sn dipole cold-mass by 2014 to demonstrate the feasibility of Nb_3Sn technology for this LHC upgrade. This program was initiated by the development of a 2-m-long single-aperture demonstrator magnet [4]. The goal of the second phase is the design and construction of an accelerator-quality twin-aperture demonstrator magnet of the same length.

This paper describes the two electromagnetic and mechanical designs of the 11 T twin-aperture Nb_3Sn dipole demonstrator magnet, one based on the coil with integrated poles and the collared coil design concept used in the single-aperture demonstrator [5], and the other one based on removable coil poles and the new collared coil design. The results of the electromagnetic field optimization and the preliminary structural analysis are discussed in addition to the quench protection scheme.

II. MAGNET DESIGN

The two-layer Nb_3Sn coils illustrated in Fig.1 and the electrical insulation scheme are identical to the single aperture demonstrator [4,5]. The coil cross-section was optimized using ROXIE [6] for the twin-aperture configuration to provide 11.21 T dipole field in the 60-mm bore at 11.85 kA with 20% operation margin, and geometrical field errors in the 10^{-4} level (dark blue area in Fig. 1). The coil is shown in Fig. 1. It consists of 56 turns, 22 in the inner layer and 34 in the outer layer. Both layers are wound from a single length of 14.7 mm wide and 1.27 mm thick keystoned Rutherford-type cable insulated with 0.15-mm-thick insulation. The cable [7,8] is made of 0.7 mm Nb_3Sn RRP-108/127 strand produced by Oxford SC Technologies (OST) using the Restack Rod Process. The strand nominal critical current density J_c(12 T,4.2 K) is 2750 A/mm^2 and the nominal Cu-fraction is 0.53.

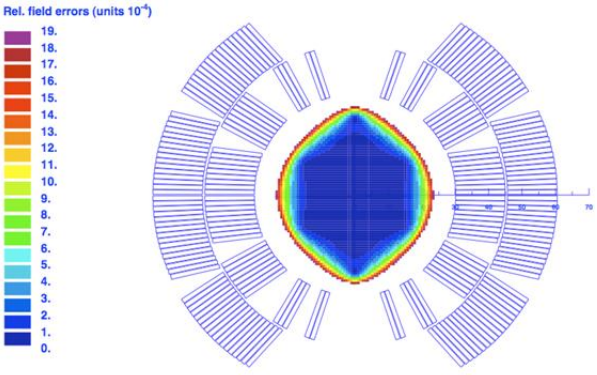

Fig. 1. Coil cross-section with geometrical field errors in units.

The mechanical structure comprises separate stainless steel collars for each aperture and a vertically split iron yoke, surrounded by a welded stainless steel outer shell. The integration in the LHC and the use of existing tooling at CERN require that the outer diameter of the iron yoke, the heat-exchanger location, and the slots for the bus-bars be identical to the MB yoke.

Manuscript received 12 September 2011. This work was supported in part by Fermi Research Alliance, LLC, under contract No. DE-AC02-07CH11359 with the U.S. Department of Energy.

B. Auchmann, M. Karppinen, L. Rossi, D. Smekens, are with CERN TE-Department, Geneva, 1211 Switzerland (phone: +41 22 767 4305; e-mail: mikko.karppinen@cern.ch).

N. Andreev, G. Apollinari, E. Barzi, R. Bossert, V.V. Kashikhin, A. Nobrega, I. Novitski, A.V. Zlobin, are with Fermilab National Accelerator Laboratory, Batavia, IL 60510 USA.

The single-aperture demonstrator coils feature integrated Ti-6Al-4V (Grade 5) poles that are potted with the coils. To provide sufficient coil pre-load at the poles this concept relies on coil mid-plane shimming and predominantly horizontal deformation of the collared coils during the cold mass assembly. As an alternative for this concept, a design with removable poles, allowing the loading of the coils at the poles similarly to the conventional collared Nb-Ti accelerator magnets and some earlier Nb_3Sn dipoles [8,9], has been analyzed for the twin-aperture demonstrator. The electromagnetic and structural optimization of these two design variants, integrated and removable pole designs are discussed below.

A. *Magnetic design*

The main electromagnetic design challenges of the twin-aperture 11 T dipole are to match the MB transfer function, to control the magnetic cross-talk between apertures, and to minimize the magnitude and variation of unwanted multipoles.

The electromagnetic models of the two yoke designs are shown in Fig. 2. The collar thickness and the outer contour of the collared coil in the regions of the yoke-collar interface are defined by the structural analysis. The main magnet parameters for both electromagnetic designs are summarized in Table 1.

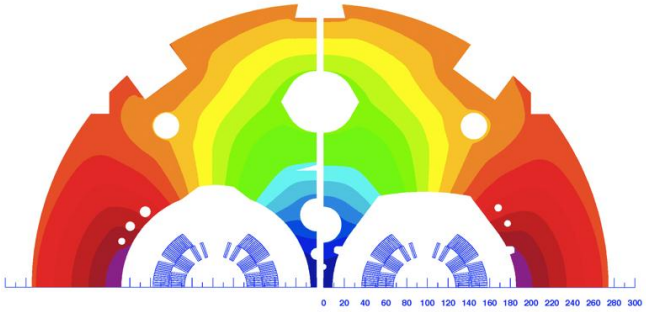

Fig. 2. Magnetic vector potential in the magnetic models optimized for the removable (left) and integrated (right) pole design.

TABLE 1 MAGNET DESIGN PARAMETERS AT 1.9 K

Parameter	Removable Pole Design	Integrated Pole Design
Nominal current I_{nom}, kA	11.85	11.85
Nominal bore field, T	11.23	11.25
Maximum coil field, T	11.59	11.60
Magnetic length, mm	1.537	1.540
Working point on the load-line at I_{nom}	81%	81%
Ultimate design field, T	12	12
Diff. inductance at I_{nom}, mH/m	11.97	11.98
Stored energy at I_{nom}, kJ/m	966.3	968.6
F_x per quadrant at I_{nom}, MN/m	3.15	3.16
F_y per quadrant at I_{nom}, MN/m	-1.58	-1.59
Fz per aperture, kN	430	430
Overall length, mm	1960	1960
Coil overall length, mm	1760	1760
Yoke outer diameter, mm	550	550
Outer shell thickness, mm	10	10
Mass, kg	~2600	~2600

The nature of the magnetic flux pattern in the 2-in-1 yoke configuration requires additional features to minimize the cross-talk between the apertures, in particular for the b_2 component. The two holes in the yoke insert reduce the b_2 variation from 16 units to 13 and 11 units in the case of the removable pole and integrated pole designs, respectively. Such large cross-talk indicates that the distance between the apertures and the overall size of the yoke would need to be increased for such a high field magnet.

In dipole magnets the iron saturation typically gives raise to variation of the b_3 and b_5 components. The shape of the cut-out on top of the aperture was optimized to reduce the saturation effects, e.g. the b_3 variation by 4.7 units as compared to a circular shape. In addition to the holes in the yoke insert, an array of three smaller holes and the position of the hole for the tie-rods were used to further reduce the b_3 variation by 2.4 units such that the iron saturation induced variation of b_3 and b_5 is 0.51 and 0.35 units, respectively, between injection and nominal current for the removable pole design. Similarly, for the integrated pole design, based on single aperture demonstrator collars, the b_3, and b_5 variation were optimized to 0.02 and 0.06 units, respectively. In this case the radius on top of the aperture was the key optimization parameter to reduce the b_3 variation.

To limit the field enhancement in the end regions the 110 mm cut-back length of the magnetic iron was defined such that peak field in the coil is located in the straight section. This results in slightly higher cross-talk between the apertures in the end region. Consequently, the integrated b_2 component in the 2-m-long demonstrator magnet is calculated to be -15.8 units, as compared to -12.2 units in the straight-section.

Table 2 lists the calculated transfer functions and expected field harmonics including iron saturation and magnetization effects for the 2-m-long demonstrator magnet at injection current (I_{inj}) of 757 A and at the nominal operation current of 11.85 kA. This analysis was carried out using the nominal LHC powering pre-cycle [2] and the reset current (I_{res}), the lowest current in the pre-cycle, of 350 A.

TABLE 2 TRANSFER FUNCTION AND FIELD HARMONICS (IN UNITS 10^{-4}) IN THE STRAIGHT SECTION AT R_{REF}=17 MM AND I=757 A / I = 11850 A, WITH SC MAGNETIZATION EFFECTS

Parameter	Removable Pole Design		Integrated Pole Design	
	757 A	11850 A	757 A	11850 A
B_1/I, T/kA	1.001	0.947	1.010	0.949
b_2	0.21	-12.22	0.13	-7.14
b_3	43.51	4.80	44.51	6.04
b_4	-0.07	-0.47	0.05	-0.44
b_5	4.54	0.28	0.01	-0.02
b_7	0.08	0.03	0.04	0.02
b_9	0.18	0.96	0.19	0.96

The coil magnetization effects in the 11 T Nb_3Sn dipoles are expected to be significantly greater than in the present Nb-Ti dipoles (MB) [4]. Recent beam optics studies for the LHC upgrade [11] suggest that sextupole errors of up to some ±20 units at injection energy can be tolerated without compromising the dynamic aperture of the machine. The calculated b_3 component due to the persistent currents in the 11 T dipole is about 44 units at the LHC injection current. The magnetization effect strongly depends on the current pre-cycle as shown in Fig. 3. Using I_{res} = 100 A the sextupole component can be reduced to stay within ±20 units between I_{inj} and I_{nom}. Possible passive correction schemes are being studied to further reduce the field harmonics at low fields [12].

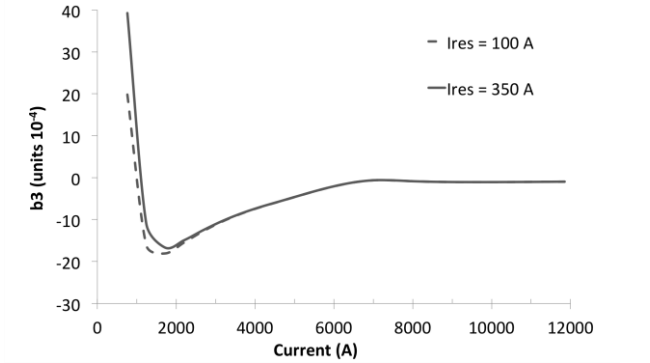

Fig.3. Calculated sextupole variation due to magnetization effects with various powering pre-cycles with I_{res} = 350 A and I_{res} = 100 A.

In the LHC a pair of 5.5-m-long 11 T dipoles is foreseen to be powered in series with the MB-magnets and this pair shall provide the same integrated strength of 119 Tm at the nominal current of 11.85 kA. Due to stronger iron saturation effect, the Nb_3Sn dipoles will be stronger than the MB at lower excitation levels, the peak difference being 2.4 Tm at 6.7 kA as shown in Fig. 4. This can be compensated either by additional orbit correctors or with 300 A bi-polar trim power converters across the 11 T dipoles.

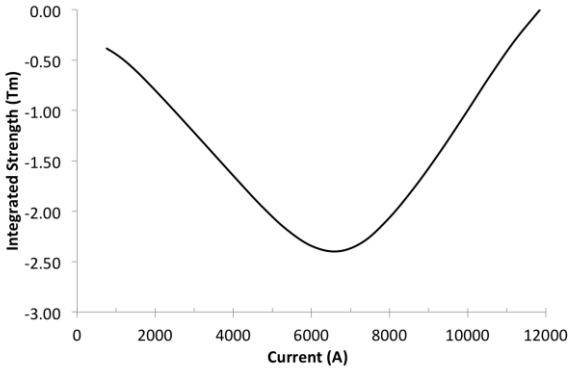

Fig. 4. Difference in the integrated strength of a pair of 5.5-m-long 11 T dipoles and the MB with both delivering 119 Tm at 11.85 kA. At lower excitation levels the 11 T dipole is stronger than the MB.

B. Mechanical design

The goal of the mechanical design is to provide a rigid clamping of the superconducting coil with minimum distortion of the conductor positioning, whilst maintaining the stresses at an acceptable level at all times. A detailed structural analysis was carried out on both design concepts to explore the optimal parameter space for the magnet assembly. The fully parametric finite element models of the integrated and removable pole designs are illustrated in Fig. 5. Both designs feature separate collared coils inside a vertically split yoke made in three parts (two separate half yokes and a solid central yoke insert).

1) Removable pole design

This design concept is inspired by the MFISC [13] model and the collar thickness was chosen for maximum rigidity in the available space to minimize the spring-back effect after the collaring process. The removable pole allows the adjustment of the coil pre-compression at the poles. An additional Cu-alloy filler wedge, which is potted together with the coil, is added to the outer layer to match the azimuthal size of the inner layers to simplify the pole wedge geometry as shown in Fig. 6. To protect the fragile Nb_3Sn coils during the collaring process a stainless steel loading plate is located between the potted coil and the pole wedge. In the collared coil the stress pattern can be tuned by varying the thickness of the shims at the pole and at the mid-plane. This gives an optimal stress distribution when then the magnet is powered by limiting the mid-plane stress while keeping the poles under compression. The pole shim is gradually reduced in the end regions to avoid a discontinuous stress pattern in the coils. The layer-jump is also integrated into the filler wedge and the loading plate.

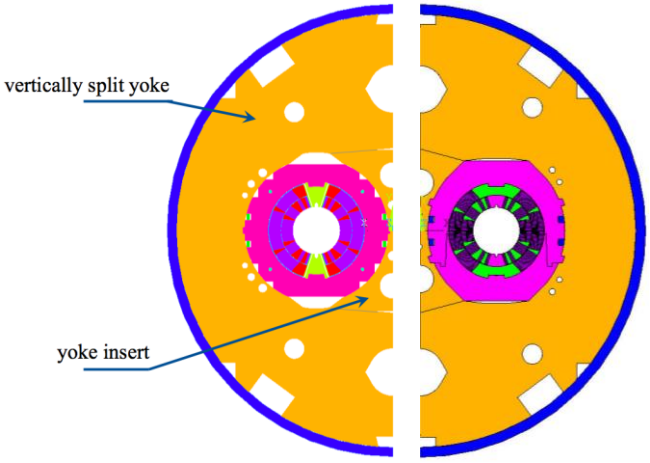

Fig. 5. FE-models of the removable (left) and integrated (right) pole designs.

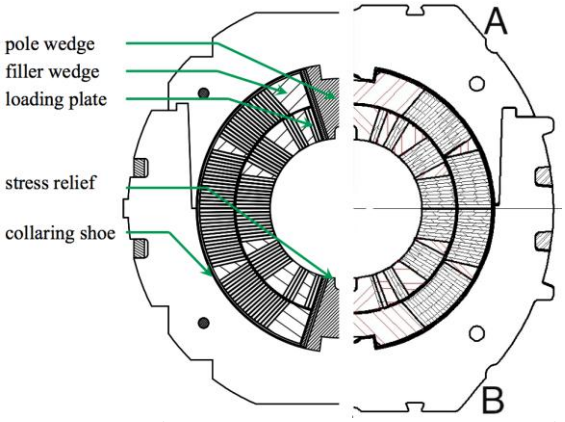

Fig. 6. Cross-section of a collared-coil assembly with removable (left) and integrated (right) poles.

The collared coils are assembled between the yoke halves and the central yoke insert, and the 10-mm-thick stainless steel outer half shells. The assembly is welded together within the welding press resulting in about 275 MPa maximum tensile shell stress. Increasing the shell thickness to 12 mm would reduce this to ~230 MPa. The yoke inner radius is 0.115 mm larger than the collar outer radius and there is a horizontal offset of 0.135 mm between centers of the yoke and the collar radii. This increases the radial interference between the somewhat deformed collared coil assembly and the yoke by 0.020 mm, thus minimizing the elliptic deformation of the coils, which reduces the sensitivity for assembly tolerances and improves the field quality. This interference is also important to maintain the contact between the yoke and the collared coil at the operation temperature. The yoke gap is closed at room temperature and remains closed up to 12 T field in the bore. Table 3 lists the evolution of the coil stress during the fabrication process, at the operation temperature, and during the excitation. The poles remain under compression at all times and maximum coil stress is under 145 MPa.

2) Integrated pole design

The coils in the single-aperture demonstrator model have integrated (potted) poles made of Ti alloy [5]. In this analysis the coil outer-layer poles are made of stainless steel while the inner-layer poles are Ti to achieve better stress distribution between inner and outer layers after cooling-down.

The required coil pre-stress in the twin-aperture demonstrator dipole is created in several steps. The initial pre-loading is obtained by ~0.100 mm mid-plane and 0.025 mm radial shims during the collaring of the coils. The maximum achievable pre-stress in the pole region is limited at this stage by the maximum coil stress near the mid-plane. During the cold mass assembly the coil pole pre-stress is increased by horizontal deformation of the collared coils (coil bending) utilizing ~0.125 mm horizontal collar-yoke interference. This interference also provides the collar-yoke contact after the cool-down. The vertical gap between the two yoke halves stays open at room temperature and it is controlled by the precise collar dimensions near the top and bottom horizontal surfaces of the collared coil (A and B in Fig. 6). Due to larger thermal contraction of the stainless steel outer shell and the collared coil relative to the iron yoke, the gap is closed during the cool-down to 1.9 K and stays closed up to the ultimate design field of 12 T. The maximum tensile stress in 10-mm-thick shell from the FEA was 320 MPa. Increasing the shell thickness to 12 mm would reduce this to approximately 280 MPa.

3) Results and discussion

The maximum coil pre-stress in the pole and mid-plane areas after collaring, cold mass assembly, cooling down to the operation temperature and at the ultimate design field of 12 T are summarized in Table 3. Diagrams of stress distribution in coil after assembly inside the 2-in-1 yoke at room temperature, after cool-down, and at 12 T for coils with removable and integrated poles are shown in Fig. 7.

Despite of the iron yoke asymmetry with respect to the vertical planes in each collared coil the stress distribution inside collared coils is quite symmetric in both design approaches. The poles remain under compression at all times and maximum coil stress remains below 150 MPa.

C. Quench protection

Magnet protection in accelerators in case of a quench is provided by heaters. To provide the reliable heater insulation quench protection heaters composed of stainless steel strips are placed between the 2nd and 3rd Kapton layers of ground insulation, covering the outer-layer coil blocks. The heater strips on each side of each coil are connected in series forming two heater circuits connected in parallel. The results of preliminary quench analysis suggests that a redundant quench protection system with outer-layer heaters must rely on highly efficient protection heaters. Experimental studies and optimization of the protection heaters are a key part of the demonstrator magnet test program.

III. Conclusion

The electromagnetic design of the twin-aperture 11 T dipole magnet meets the requirements of the LHC collimation upgrade. The structural analysis demonstrates that the coils can be rigidly clamped at all times up to 12 T field whilst keeping the stresses at acceptable levels. The final mechanical concept for the twin-aperture magnet will be selected later based on the results from more detailed finite element analysis and experimental studies on short mechanical models.

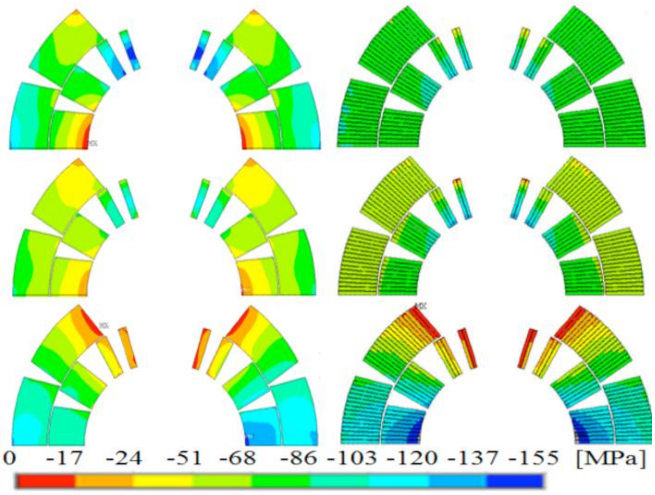

Fig. 7. Azimuthal stress distribution in the coils after the cold mass assembly at room temperature (top), after cool-down (middle) and at 12 T (bottom) for removable pole (left) and integrated pole (right) designs.

TABLE 3 Maximum Azimuthal Coil Pre-Stress in Pole and Mid-Plane Regions

Collar/coil design	Position in coil	Azimuthal Coil Stress, MPa				
		Under press	Collared coil	Cold mass	Cool down	B=12T min/max
Removable poles	Inner pole	-126	-92	-143	-115	-27/-5
	Outer pole	-87	-52	-65	-61	-37/-5
	Inner midplane	-115	-55	-65	-58	-134
	Outer midplane	-91	-66	-95	-94	-127
Integrated poles	Inner pole	-69	-54	-108	-124	-7/0
	Outer pole	-97	-65	-70	-50	-14/0
	Inner midplane	-148	-102	-71	-67	-136
	Outer midplane	-79	-55	-78	-66	-116

References

[1] L. Rossi et al., "Advanced Accelerator Magnets for Upgrading the LHC", *this conference*.

[2] O. Brüning, P. Collier, P. Lebrun, S. Myers, R. Ostojic, J. Pool, and P. Proudlock. LHC design report volume 1 the LHC main ring. Technical report, CERN, June 2004.

[3] G. de Rijk, A. Milanese, E. Todesco, "11 Tesla Nb3Sn dipoles for phase II collimation in the Large Hadron Collider", sLHC Project Note 0019, 2010.

[4] A.V. Zlobin et al., "Development of Nb_3Sn 11T Single Aperture Demonstrator Dipole for LHC Upgrades", Fermilab-Conf-11-126-TD, PAC'2011, NYC, March 2011.

[5] A.V. Zlobin et al., "Design and Fabrication of a Single-Aperture 11T Nb_3Sn Dipole Model for LHC Upgrades", *this conference*.

[6] ROXIE, http://espace.cern.ch/roxie.

[7] E. Barzi et al., "Nb3Sn Cable Development for the 11 T Dipole Demonstration Model", CEC/ICMC'2011, Spokane, WA, June 2011

[8] E. Barzi et al., "Development and Fabrication of Nb_3Sn Rutherford Cable for the 11 T DS Dipole Demonstration Model", *this conference*.

[9] A. Asner et al., "First Nb_3Sn, 1 m Long Superconducting Dipole Model Magnets for LHC break the 10 Tesla Field Threshold", proceedings of MT-11, Tsukuba, Japan, 1989.

[10] A. den Ouden et al., "An Experimetnal 11.5 T Nb_3Sn LHC Type Dipole Magnet", IEEE Trans. Mag. Vol. 30, 1994, p.2320.

[11] B. Holzer CERN BE-ABP-LCU, private communication June 2011.

[12] E. Barzi, D. Chichili, J. DiMarco, V.V. Kashikhin, M. Lamm, P. Schlabach, A.V. Zlobin, "Passive correction of the persistent current effect in Nb3Sn accelerator magnets", IEEE Transactions on Applied Superconductivity, Vol. 13, No. 2, June 2003, pp.1270-1273.

[13] J. Ahlbäck et al., "Electromagnetic and Mechanical Design of a 56 mm Aperture Model Dipole for the LHC", IEEE Trans. on Magnetics, July 1994, vol 30, No. IV, pp. 1746-174.